BRNO UNIVERSITY OF TECHNOLOGY
VYSOKÉ UČENÍ TECHNICKÉ V BRNĚ

FACULTY OF INFORMATION TECHNOLOGY
FAKULTA INFORMAČNÍCH TECHNOLOGIÍ

DEPARTMENT OF COMPUTER GRAPHICS AND MULTIMEDIA
ÚSTAV POČÍTAČOVÉ GRAFIKY A MULTIMÉDIÍ

DESIGN OF GUIDANCE, NAVIGATION AND CONTROL FOR VERTICAL LANDING OF A REUSABLE ROCKET BOOSTER

NÁVRH NAVEDENÍ, NAVIGACE A ŘÍZENÍ PRO VERTIKÁLNÍ PŘISTÁNÍ OPAKOVANĚ POUŽITELNÉHO RAKETOVÉHO URYCHLOVAČE

MASTER'S THESIS
DIPLOMOVÁ PRÁCE

AUTHOR **Bc. ADRIÁN KIRÁLY**
AUTOR PRÁCE

SUPERVISOR **doc. Ing. PETER CHUDÝ, Ph.D., MBA**
VEDOUCÍ PRÁCE

BRNO 2020

Brno University of Technology
Faculty of Information Technology

Department of Computer Graphics and Multimedia (DCGM) Academic year 2020/2021

Master's Thesis Specification

Student: **Király Adrián, Bc.**
Programme: Information Technology and Artificial Intelligence Specialization: Computer Graphics and Multimedia
Title: **Design of Guidance, Navigation and Control for Vertical Landing of a Reusable Rocket Booster**
Category: Modelling and Simulation
Assignment:

1. Create a dynamic model and research aerodynamic characteristics of a reusable rocket booster.
2. Get familiar with the design of spacecraft guidance, navigation and control system.
3. Design and create a Matlab implementation of guidance, navigation, and control for vertical landing of the booster.
4. Implement a visualization environment for an intuitive interpretation of the computed landing trajectory.
5. Evaluate achieved results and discuss potential further improvements.

Recommended literature:

- According to supervisor's recommendations.

Requirements for the semestral defence:

- Items No. 1, 2 and partially item No. 3.

Detailed formal requirements can be found at https://www.fit.vut.cz/study/theses/

Supervisor: **Chudý Peter, doc. Ing., Ph.D. MBA**
Head of Department: Černocký Jan, doc. Dr. Ing.
Beginning of work: November 1, 2020
Submission deadline: May 19, 2021
Approval date: October 30, 2020

Abstract

This work describes the theoretical basis for developing guidance, navigation, and control system for the vertical landing of a reusable rocket booster. The final result of this work will be a sufficiently realistic simulation of the landing phase.

Abstrakt

Táto práca popisuje teoretické východiská pre vývoj systému pre navádzanie, navigáciu, a riadenie pre vertikálne pristátie znovupoužiteľného raketového urýchľovača. Finálnym výsledkom tejto práce bude dostatočne realistická simulácia pristávacej fázy.

Keywords

reusable rocket booster, vertical landing, guidance, aerodynamics, controls, simulation, GNC

Kľúčové slová

znovupoužiteľný raketový urýchľovač, vertikálne pristátie, navádzanie, aerodynamika, riadenie, simulácia, GNC

Reference

KIRÁLY, Adrián. *Design of Guidance, Navigation and Control for Vertical Landing of a Reusable Rocket Booster*. Brno, 2020. Master's thesis. Brno University of Technology, Faculty of Information Technology. Supervisor doc. Ing. Peter Chudý, Ph.D., MBA

Rozšírený abstrakt

Abstract

Design of Guidance, Navigation and Control for Vertical Landing of a Reusable Rocket Booster

Declaration

Hereby I declare that this bachelor's thesis was prepared as an original author's work under the supervision of doc. Ing. Peter Chudý, Ph.D., MBA. All the relevant information sources, which were used during preparation of this thesis, are properly cited and included in the list of references.

.....
Adrián Király
April 23, 2021

Acknowledgements

I would like to thank my supervisor doc. Ing. Peter Chudý, Ph.D., MBA for his excellent guidance and invaluable feedback and advice during my work on this master's thesis.

Contents

Todo list

List of Figures

List of Tables

Chapter 1

Introduction

For more than 60 years, humanity has relied on conventional, expendable rocket launchers to deliver payloads and people to space. However, as each of those rockets was essentially single-use, the cost of getting to space has been exceptionally high for a long time.

There were multiple attempts to resolve this issue throughout history, most notably the *Space Shuttle*. While it became the first reusable vehicle to reach orbit, it never fulfilled its aim of reducing the cost of getting to space.

citation needed

Another notable project was the *McDonnell Douglas DC-X*, which was one of the first working prototypes of a Vertical Takeoff, Vertical Landing (VTVL) vehicle. Unlike the Shuttle, it resembled conventional multi-stage rockets, but after liftoff, it landed vertically back to earth.

More than 20 years later, the vision of the DC-X project became a reality, when the first stage of *SpaceX Falcon 9* successfully landed back to Earth after delivering its payload to orbit.

The aim of this work is to design and develop a Guidance, Navigation, and Control (GNC) system of such vehicle using a software simulation of the vehicle and its environment. This is a complex task that requires the development of multiple interdependent parts and knowledge of various areas of aerospace engineering and of modeling and simulation.

The first part is a dynamic model of the rocket, which will be presented in chapter 2. This chapter also covers coordinate systems and other prerequisites for the whole work.

As the booster of a reusable rocket spends a large portion of its flight in denser parts of Earth's atmosphere, it is necessary to consider the aerodynamic characteristics of the booster, which are described in chapter 3.

The chapter 4 describes state-of-the-art in GNC design for spaceraft, which serves as a basis for building the GNC system in this work.

Chapter 2

Dynamic Model of a Reusable Rocket Booster

The first step in building the GNC system for the rocket booster is to create a mathematical model of the booster itself. This makes it possible to develop the system and simulate its function without the need for building the rocket and performing (often very expensive) real-world experiments.

In the beginning of the section, several coordinate systems will be described. These coordinate systems are necessary not only for developing the dynamic model of the booster, but will be used throughout the work. Then, the kinematic equations will be described, and lastly, the dynamic model of the rocket will be built in form of equations of motion.

2.1 Coordinate Systems and Transformations

To describe the position and movement of a rocket (or any other object), it is necessary to establish a suitable coordinate system. However, a single coordinate system may not be sufficient for all purposes. In some cases, the use of a different coordinate system may simplify certain calculations, or it may be a natural way to express certain phenomena [6]. This, however, makes it necessary to perform transformations between various coordinate systems.

This section will introduce several reference frames and coordinate systems that will be used in this work. These definitions are in line with the coordinate systems used by the MATLAB Aerospace Toolbox [27]. Furthermore, the transformations between consecutive systems will be presented, making it possible to build a transformation between any two coordinate systems.

2.1.1 Earth-Centered Inertial Frame

In general, an inertial reference frame is a frame of reference that is not rotating or accelerating. The Earth-Centered Inertial frame (ECI) (see fig. 2.1) is a global frame with the origin at Earth's center of mass and fixed relative to the stars, which means the Earth's rotation can be observed in this frame. This makes it a preferred frame for describing the motion of a spacecraft in near-Earth environments [8].

The ECI frame is defined as follows [8]:

- The origin o_I is at the center of mass of the Earth.

- The x_I axis is pointing towards the vernal equinox (a point at which the ecliptic intersects the celestial equator [1]).
- The z_I axis is parallel to the Earth's rotation axis, pointing towards the Conventional Terrestrial Pole (CTP).
- The remaining y_I axis completes the right-handed coordinate system.

The equatorial plane and the ecliptic slightly move over time, which means the position of the vernal equinox changes [30]. To define a truly inertial frame, the position of the vernal equinox must be fixed. This is achieved by referring to its position at a particular point in time. Most commonly, the *J2000.0 Epoch* is used, which refers to January 1, 2000, at 12:00 Terestrial Time (TT).

2.1.2 Earth-Centered, Earth-Fixed Frame

The Earth-Centered, Earth-Fixed frame (ECEF), shown in fig. 2.1, is similar to the ECI frame, as it has the same origin and z-axis. The major difference is that ECEF is co-rotating with the Earth, which means that the coordinates of a given point do not change over time.

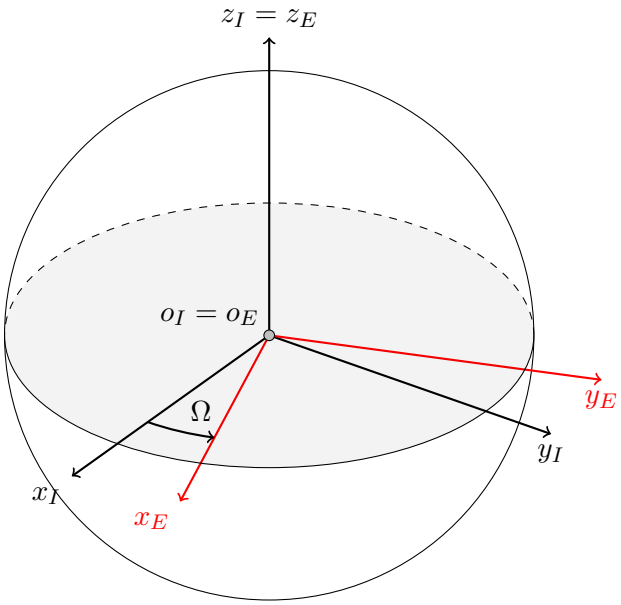

Figure 2.1: The Earth-Centered Inertial frame and Earth-Centered, Earth-Fixed frame are related through a single rotation by angle Ω.

The full definition of the ECEF frame is following [16]:

- The origin o_E is at the center of mass of the Earth.
- The x_E axis is pointing towards the intersection of the prime meridian and the equatorial plane.
- The z_E axis is parallel to the Earth's rotation axis, pointing towards the CTP.
- The remaining y_E axis completes the right-handed coordinate system.

As can be seen from fig. 2.1, the ECEF and ECI frames are related by a rotation around a single axis ($x_E = x_I$), and the angle Ω of the rotation is a linear function of time [8].

Transformation from ECI to ECEF

The size of the angle Ω is dependent on the angular speed of the Earth ω_{Earth} and the time elapsed since the J2000.0 Epoch [8]:

$$\Omega = \omega_{Earth}(t - t_{J2000}) \tag{2.1}$$

The angular speed of the Earth is defined as [8]:

$$\omega_{Earth} = 7.292\,115\,167 \times 10^{-5} \mathrm{rad\,s^{-1}} \tag{2.2}$$

We can then construct a transformation matrix $\boldsymbol{T_I^E}$ for transformation from ECI to ECEF as a rotation $\boldsymbol{R_{z_E}}(\Omega)$ around the z_E axis by angle Ω:

$$\boldsymbol{T_I^E} = \boldsymbol{R_{z_E}}(\Omega) = \begin{bmatrix} \cos\Omega & \sin\Omega & 0 \\ -\sin\Omega & \cos\Omega & 0 \\ 0 & 0 & 1 \end{bmatrix} \tag{2.3}$$

2.1.3 Local Geographic Frame

The Local Geographic Frame is an intuitive frame suitable for cases when the vehicle is on or near the Earth's surface, as it represents the Earth's surface as a flat plane tangent to a given point on Earth (see fig. 2.2. This assumption is adequate mostly in scenarios whose total extent is smaller than some tens of kilometers [13].

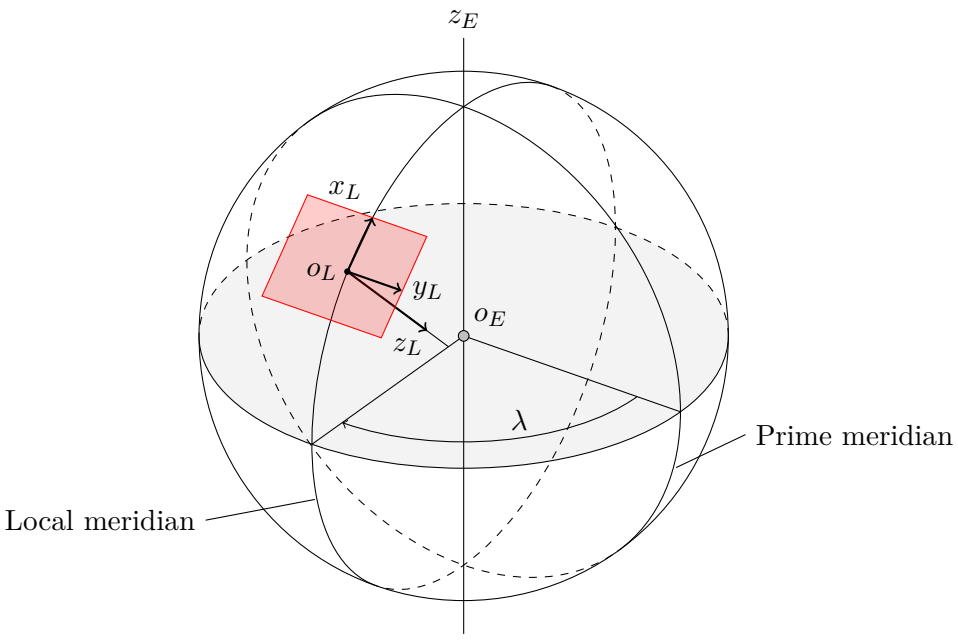

Figure 2.2: The Local Geographic Frame and North-East-Down coordinate system.

There are multiple ways to define axes in a local geographic frame. The most commonly used definition in aerospace is the North-East-Down (NED) coordinate system (depicted in fig. 2.2), defined as follows [13]:

- The origin o_L is fixed to a given point on the surface of the Earth.
- The x_L axis points towards the north, parallel to the local horizontal plane.
- The y_L axis points towards the east, parallel to the local horizontal plane.
- The z_L axis points vertically down.

Add text about (Geodetic) latitude/longitude

Transformation from ECEF to NED

Assume that $\boldsymbol{P_E}$ is a position in ECEF coordinate system and $\boldsymbol{P_r}$ is the position of the NED coordinate system origin (o_L). Then, the position of the point $\boldsymbol{P_E}$ can be transformed to NED coordinates $\boldsymbol{P_L}$ using the following equation [3]:

$$\vec{P_L} = \boldsymbol{T_E^L}\left(\vec{P_E} - \vec{P_r}\right) \tag{2.4}$$

The transformation matrix $\boldsymbol{T_E^L}$ is given by [3]:

$$\boldsymbol{T_E^L} = \begin{bmatrix} -\sin\Phi_r\cos\lambda_r & -\sin\Phi_r\sin\lambda_r & \cos\Phi_r \\ -\sin\lambda_r & \cos\lambda_r & 0 \\ -\cos\Phi_r\cos\lambda_r & -\cos\Phi_r\sin\lambda_r & -\sin\Phi_r \end{bmatrix} \tag{2.5}$$

2.1.4 Body Fixed Frame

To describe the orientation of a vehicle relative to its initial position, a sequence of rotations around the roll, pitch, and yaw axes is commonly used [8]. The angles of these rotations are called the *Euler angles*. It is important to preserve the order of rotations, as applying rotations in an incorrect order may result in a different vehicle orientation.

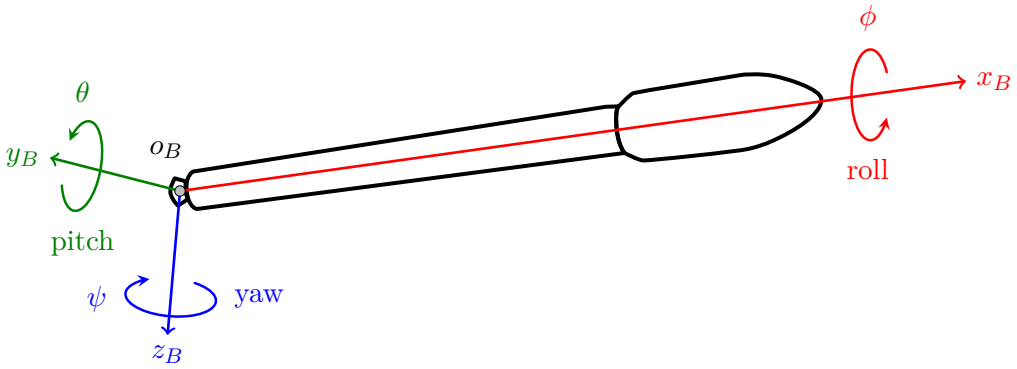

Figure 2.3: The Body Fixed Frame.

These axes also form the Body Fixed Frame (BFF) (see fig. 2.3) of the vehicle. This frame is also the frame-of-choice for specifying the positions of various internal components and other significant points inside the rocket.

The exact definition of the frame may be slightly different on some launch vehicles, but generally, the following definition applies [14, 23]:

- The origin o_B lies at a fixed place along the longitudinal axis of the vehicle. For launch vehicles, the origin is usually situated below the gimbal plane of the stage.

- The x_B axis is aligned with the longitudinal axis and points towards the nose.
- The y_B axis usually points towards a certain significant feature on the surface of the rocket (such as the fin).
- The z_B axis completes the right-handed coordinate system.

Transformation from NED to BFF

If we coincide the origins of the NED and BFF coordinate systems to same point $o = o_L = o_B$, then we can formulate the transformation matrix T_L^B from NED to BFF as [3]:

$$\begin{aligned} \boldsymbol{T_L^B} &= \boldsymbol{R_1}(\phi)\,\boldsymbol{R_2}(\theta)\,\boldsymbol{R_3}(\psi) \\ &= \begin{bmatrix} \cos\theta\cos\psi & \cos\theta\sin\psi & -\sin\theta \\ \sin\phi\sin\theta\cos\psi - \cos\phi\sin\psi & \sin\phi\sin\theta\sin\psi + \cos\phi\cos\psi & \sin\phi\cos\theta \\ \cos\phi\sin\theta\cos\psi + \sin\phi\sin\psi & \cos\phi\sin\theta\sin\psi - \sin\phi\cos\psi & \cos\phi\cos\theta \end{bmatrix} \end{aligned} \tag{2.6}$$

where ϕ, θ, ψ denote the roll, pitch, and yaw angles of the vehicle, respectively.

2.2 Kinematic Differential Equations

The Kinematic Differential Equations deal with the time-dependent relationship between two reference frames [29]. In other words, these equations describe how the relative orientation of two frames changes over time. It is important to note that kinematics study the orientation of the body without involving any of the forces acting on the body, and as such, the relations presented in this section are purely mathematical [29].

There are multiple ways to express the orientation of the body, which also means that there are different ways to express the kinematic differential equations. The most intuitive one is using the *Euler angles*. While it is a simple-to-understand method, it has one significant limitation, which can be resolved using a quaternion expression of the kinematic equation.

2.2.1 Euler Angles

Total angular velocity $\vec{\omega}$ can be expressed in terms of the basis vectors $\vec{i}, \vec{j}, \vec{k}$ of a Body Fixed Frame:

$$\vec{\omega} = p\vec{i} + q\vec{j} + r\vec{k} \tag{2.7}$$

where p, q, and r are the components of the angular velocity [29]. Then, the time derivatives of Euler angles $\dot{\phi}, \dot{\theta}, \dot{\psi}$ (roll, pitch, and yaw rates) can be related to p, q, r using a series of rotations [29]:

$$\vec{\omega} = \begin{bmatrix} \dot{\phi} \\ 0 \\ 0 \end{bmatrix} + R_x(\phi) \begin{bmatrix} 0 \\ \dot{\theta} \\ 0 \end{bmatrix} + R_x(\phi)R_y(\theta) \begin{bmatrix} 0 \\ 0 \\ \dot{\psi} \end{bmatrix} \tag{2.8}$$

Now, from eq. (2.8) we can obtain the final kinematic differential equation:

$$\begin{bmatrix} \dot{\phi} \\ \dot{\theta} \\ \dot{\psi} \end{bmatrix} = \begin{bmatrix} 1 & \sin\phi\tan\theta & \cos\phi\tan\theta \\ 0 & \cos\phi & -\sin\phi \\ 0 & \sin\phi\sec\theta & \cos\phi\sec\theta \end{bmatrix} \begin{bmatrix} p \\ q \\ r \end{bmatrix} \tag{2.9}$$

The inverse relationship can be obtained by inverting the matrix in eq. (2.9):

$$\begin{bmatrix} p \\ q \\ r \end{bmatrix} = \begin{bmatrix} 1 & 0 & -\sin\theta \\ 0 & \cos\phi & \sin\phi\cos\theta \\ 0 & -\sin\phi & \cos\phi\cos\theta \end{bmatrix} \begin{bmatrix} \dot{\phi} \\ \dot{\theta} \\ \dot{\psi} \end{bmatrix} \tag{2.10}$$

As mentioned earlier, there is a limitation when using Euler angles—the eqs. (2.9) and (2.10) become singular when $\theta = \pi/2$ [29]. This inherent property of Euler angles may not be an issue in some scenarios but can be fully resolved only by using a different representation of kinematic equations.

2.2.2 Quaternions

In short, quaternions are an extension to complex numbers with numerous applications. They are particularly suitable for working with rotations in three-dimensional space, as they both solve the issue of singularities encountered when using the Euler angles and are also computationally more efficient [12].

A rotation around a basis vector $\vec{u}$ by angle θ can be performed by first constructing a rotation quaternion in the form of

$$q = q_0 + \boldsymbol{q} = \cos\frac{\theta}{2} + \vec{u}\sin\frac{\theta}{2} \tag{2.11}$$

Subsequently, a vector $\vec{v}$ can be rotated by the following operation:

$$q\vec{v}q^* \tag{2.12}$$

where q^* is the conjugate of quaternion q defined as $q^* = q_0 - q_1\vec{i} - q_2\vec{j} - q_3\vec{k}$ [12].

As a consequence, quaternions can be used to express the kinematic equations, while gaining all of the benefits mentioned earlier. The following are the kinematic differential equations expressed with quaternions [24]:

$$\begin{bmatrix} \dot{q_0} \\ \dot{q_1} \\ \dot{q_2} \\ \dot{q_3} \end{bmatrix} = \frac{1}{2} \begin{bmatrix} 0 & -p & -q & -r \\ p & 0 & r & -q \\ q & -r & 0 & p \\ r & q & -p & 0 \end{bmatrix} \begin{bmatrix} q_0 \\ q_1 \\ q_2 \\ q_3 \end{bmatrix} \tag{2.13}$$

While quaternions are immensely useful during the calculations, they are not easy to interpret. Thus, it is often convenient to express the quaternion as Euler angles, which can be done using the following equations [20]:

$$\phi = \arctan\left(\frac{2\left(q_0q_1 + q_2q_3\right)}{q_0^2 - q_1^2 - q_2^2 + q_3^2}\right) \tag{2.14}$$

$$\theta = \arcsin\left(2\left(q_0q_2 - q_1q_3\right)\right) \tag{2.15}$$

$$\psi = \arctan\left(\frac{2\left(q_0q_3 + q_1q_2\right)}{q_0^2 + q_1^2 - q_2^2 - q_3^2}\right) \tag{2.16}$$

2.3 Equations of Motion

The equations of motion describe the translational and rotational behavior of the vehicle in time depending on the forces and moments acting on the body of the vehicle [24]. The basis of these equations is the concepts and relationships presented earlier in this chapter.

In many cases, a single plane is sufficient to describe the flight path of a rocket booster. This means that the rocket needs only 3 Degrees of Freedom (DOF), which significantly simplifies the equations of motion. However, this work utilizes all 6 DOF in simulation to accurately describe any possible case. Furthermore, as the distances covered by the rocket booster during the launch are significant, the assumption of a flat Earth is not viable for this use. Hence, the position of the vehicle is expressed using the ECEF in equations of motion.

The following equation describes the translational motion using the ECEF [24, 28]:

$$\vec{F_b} = \begin{bmatrix} F_x \\ F_y \\ F_z \end{bmatrix} = m \left\{ \dot{\vec{V}_b} + \vec{\omega_b} \times \vec{V_b} + \boldsymbol{T_E^B} \cdot \vec{\omega_e} \times \vec{V_b} + \boldsymbol{T_E^B} \cdot \left[\vec{\omega_e} \times \left(\vec{\omega_e} \times \vec{X_f} \right) \right] \right\} \tag{2.17}$$

where:

- $\vec{F_b}$ is given in the BFF,
- m is the current mass of the vehicle,
- $\vec{V_b} = \begin{bmatrix} u & v & w \end{bmatrix}^T$ is the velocity vector of the vehicle in the BFF,
- $\vec{\omega_b}$ are the angular rates with respect to ECI given in BFF,
- $\vec{\omega_e}$ is the Earth rotation rate,
- and $\boldsymbol{T_E^B}$ is the transformation matrix from the ECEF axes to BFF axes.

finish

Similarly, the rotational behavior of the rocket can be described by the following equation [24, 28]:

$$\vec{M_b} = \begin{bmatrix} L \\ M \\ N \end{bmatrix} = \vec{I}\dot{\vec{\omega}_b} + \vec{\omega_b} \times \left(\vec{I}\vec{\omega_b} \right) + \dot{I}\vec{\omega_b} \tag{2.18}$$

where the moments $\vec{M_b}$ given in the BFF are related to angular rates ω_b, and the inertia tensor I.

Chapter 3

Aerodynamic Characteristics of a Reusable Rocket Booster

The booster of a reusable rocket spends most of its time in denser layers of the atmosphere, where the effects of aerodynamic forces cannot be neglected. More importantly, it is necessary to utilize aerodynamic effects to steer the booster during its descent, as purely Reaction Control System (RCS) based approach is not sufficient and effective [5].

The beginning of this chapter will focus on the general description of aerodynamic forces and moments, and the theory related to them. Then, the process of determination of aerodynamic coefficients for the reusable rocket booster will be discussed.

3.1 Aerodynamic Forces and Moments

Among the major forces that act on the rocket during its flight in the atmosphere are the aerodynamic forces. They are mechanical forces generated by the relative motion of a rocket in the air. As such, these forces and moments depend on the orientation of the rocket relative to the airflow [24].

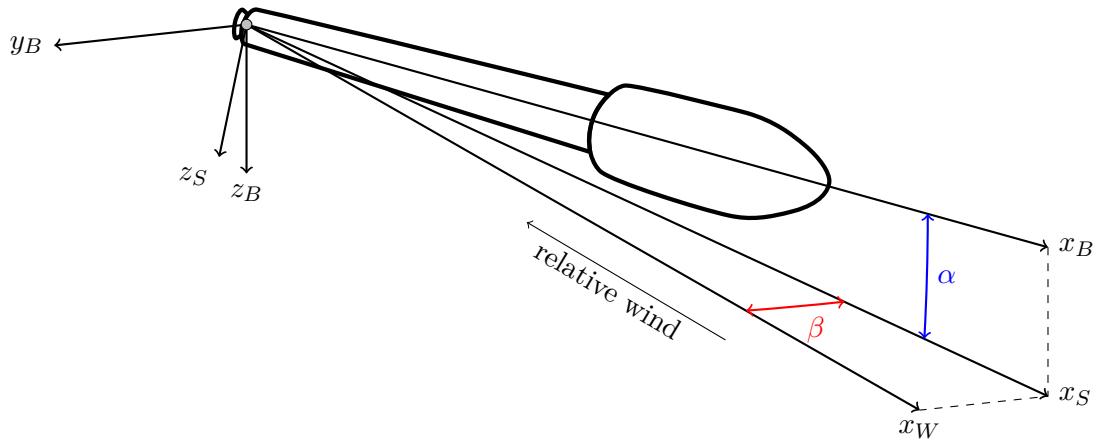

Figure 3.1: The aerodynamic angles α and β and their relation to Body Fixed Frame

To determine the aerodynamic forces and moments acting on the vehicle, it is necessary to express its orientation relative to the airflow. This is done by introducing two new coordinate systems, both originated at the same point as the BFF.

The first one is the *stability axes* coordinate system. It is obtained from the BFF by a single rotation around the y_B axis through angle α, also known as angle of attack (AoA) [24]. The second coordinate system is the *wind-axes* system, which is obtained from the stability axes by a rotation around the z_S axis. The size of this rotation is the angle of sideslip (AoS), denoted as β [24].

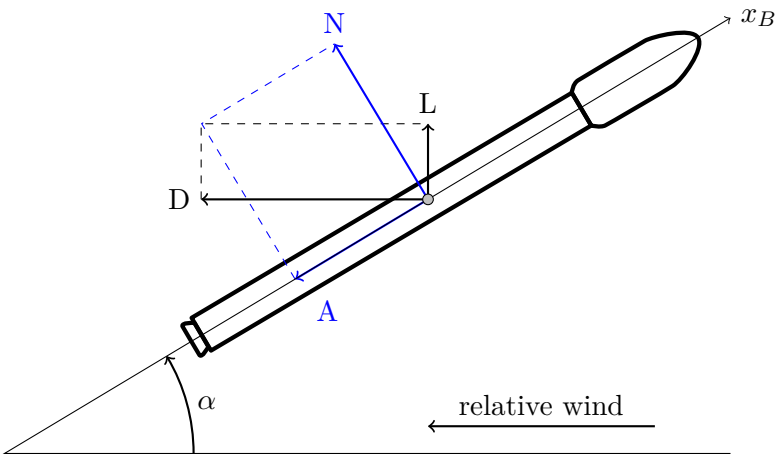

Figure 3.2: The aerodynamic forces acting on the rocket

The aerodynamic forces acting on the rocket can be decomposed into multiple components. There are several ways to perform this decomposition, which differ in the coordinate system in which are the forces decomposed, as can be seen in [22].

The most common ways of decomposition are shown in fig. 3.2. Historically, the preferred way was to express the forces in the wind-axes coordinate system as the lift force L and drag force D [22].

However, for symmetric bodies such as rockets, it is often beneficial to use the BFF to decompose the aerodynamic forces [22]. In this case, the components are the normal force N and axial force A.

As the relationship between these decompositions is purely geometrical, the components can be simply transformed using the following equations [24]:

$$N = L\cos(\alpha) + D\sin(\alpha) \tag{3.1}$$

$$A = -Lsin(\alpha) + D\cos(\alpha) \tag{3.2}$$

The inverse relation also applies:

$$L = N\cos(\alpha) - A\sin(\alpha) \tag{3.3}$$

$$D = N\sin(\alpha) + A\cos(\alpha) \tag{3.4}$$

The magnitude of the aerodynamic forces depends on the aerodynamic coefficients, which in turn depend on a large number of other variables, most importantly on the aerodynamic angles α and β, the Mach number, altitude, and others. Last, but not least, these coefficients depend on the shape of the rocket [24].

As with the forces, the aerodynamic coefficients can be also expressed in multiple coordinate systems. Equations for the transformations of these coefficients are analogous to eqs. (3.1) to (3.4). The relation between various choices of input axes and the corresponding aerodynamic coefficients can be seen in table 3.1.

Table 3.1: Aerodynamic coefficients used for various choices of axes [28].

Used axes	**Force coefficients**	**Moment coefficients**
Body	axial C_A, sideforce C_S, normal C_N	roll C_ℓ, pitch C_m, yaw C_n
Stability	drag C_D, sideforce C_S, lift C_L	roll C_ℓ, pitch C_m, yaw C_n
Wind	drag C_D, cross-wind C_C, lift C_L	roll C_ℓ, pitch C_m, yaw C_n

Assuming the coefficients are in the BFF axes, then, the aerodynamic forces A, S, N and moments ℓ, m, n are expressed by the equations [24]:

$$A = \vec{q}SC_A \tag{3.5}$$
$$S = \vec{q}SC_S \tag{3.6}$$
$$N = \vec{q}SC_N \tag{3.7}$$
$$\ell = \vec{q}SbC_\ell \tag{3.8}$$
$$m = \vec{q}ScC_m \tag{3.9}$$
$$n = \vec{q}SbC_n \tag{3.10}$$

where S, b, c are the reference area, length, and span, respectively. The quantity $\vec{q}$ is the dynamic pressure, which is effectively a product of the density ρ and square of the velocity V:

$$\vec{q} = \frac{1}{2}\rho V^2 \tag{3.11}$$

3.2 Determination of Aerodynamic Coefficients for Reusable Rocket Booster

As was shown in the previous section, the calculation of forces and moments acting on the vehicle is relatively trivial if the aerodynamic coefficients are known. Unfortunately, the values of those coefficients are highly dependent on the shape of the vehicle, aerodynamic angles, and Mach number. It is apparent that the determination of the aerodynamic coefficients is a complex task and necessitates the application of special techniques.

While the topic of the determination of aerodynamic coefficients is far out of the scope of this work, for the sake of completeness, a brief description of several methods will be presented in this section.

3.2.1 Experimental Methods

The traditional method of obtaining flight coefficients is by performing an experiment in a wind tunnel using a scaled-down model of the vehicle. During the test, the model is mounted on a rigid test fixture (commonly known as a „sting“) and the air is made to flow past the model. Using various probes and sensors, many different parameters can be measured [24].

The obvious disadvantage of this method is the time complexity and cost associated with building the scale model of the vehicle and setting up the whole experiment. Therefore, it is not viable for use in this work.

3.2.2 Computational Fluid Dynamics

Thanks to the advancements in computing power in recent years, it has become increasingly more viable (and in some cases preferable) to use computer simulations to determine the aerodynamic characteristics of a vehicle [11]. This approach is commonly known as Computational Fluid Dynamics (CFD).

In CFD, a set of nonlinear equations known as *the Navier-Stokes equations* is numerically solved. These equations, based on Newton's second law of motion and energy conservation, describe the dynamics of a fluid particle in terms of its mass, momentum, and energy [11].

To solve these equations on a computer, it is necessary to truncate the computational domain using boundary conditions and to discretize it with methods such as Finite-Difference Method (FDM) or Finite-Volume Method (FVM).

3.3 Aerodynamics of Grid Fins

Chapter 4

Design of Spacecraft Guidance, Control, and Navigation Systems

The GNC subsystem is at the heart of every rocket booster. In a nutshell, its task is to successfully achieve mission goals by following the flight trajectory that leads to the target orbit and respond to disturbances from the boosters' environment. Nowadays, with the rise of reusable launch systems, its purpose is extended with the secondary task of safely landing the rocket booster back to the surface of the Earth.

The acronym GNC is an all-encompassing term covering a broad range of subsystems [18]. The **Guidance** part refers to systems responsible for the establishment of the trajectory the booster needs to follow. The purpose of **Navigation** is to find the current position of the vehicle and predict a future state. Finally, **Control** refers to the determination of actions necessary to match the current state (obtained by navigation) with the desired path (guidance). The following sections will focus on all three aspects of the GNC subsystem, their components, and the algorithms they use.

4.1 Guidance

The task of the guidance is to calculate the path the rocket needs to follow to reach a specific target. In expendable rockets, it is only necessary to determine the trajectory for reaching the target orbit. For the sake of completeness, a brief description of the launch trajectory is included in this section.

However, a reusable rocket booster also needs guidance to the landing site on the surface of the Earth. This task is much more challenging than it appears, mostly due to the extreme conditions the vehicle goes through during landing, and very tight margins for error. An algorithm for the calculation of the optimal landing path will be described later in this section.

4.1.1 Launch Trajectory

Determination of the launch trajectory is a complex optimization problem. To find an optimal solution, it is necessary to consider a large number of factors and constraints, determined by both the mission requirements (such as the target orbit) and the design and construction of the launch vehicle [19]. Despite the complexity of this task, all vertically launched launch vehicles (LVs) follow a common pattern during their ascent, which can be seen in fig. 4.1.

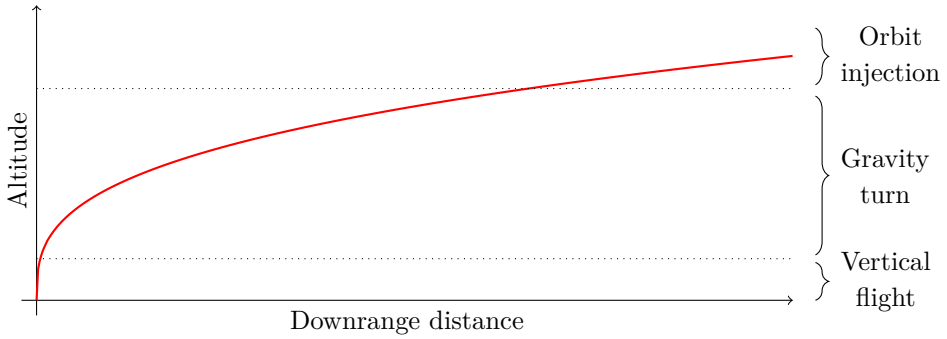

Figure 4.1: Launch trajectory of a vertically launched launch vehicle

Mention pitch kick?

The LV is accelerated vertically from the launch site and remains in vertical (or near-vertical flight) for the first roughly 15 s, during which the vehicle ascends through the denser parts of the atmosphere [19].

Due to the aerodynamic heating considerations, any turn maneuvers are usually performed when the vehicle leaves the denser atmosphere [29]. Then, the vehicle initiates a pitch maneuver, which puts it into a *gravity-turn* trajectory.

In the *gravity-turn* trajectory, the thrust vector is kept in the direction opposite to the velocity vector and the AoA is close to zero. This lowers the aerodynamic stress, making it possible to minimize the structural mass of the vehicle [29].

During the ascent, the vehicle reaches a point called *Max Q*, when it is subjected to maximum dynamic pressure [19]. Most LVs temporarily throttle down during this phase to reduce the aerodynamic loads produced on the vehicle [26].

The last step of the launch is the final guidance using the upper stage engines into the target orbit, which occurs after the vehicle leaves the atmosphere [19].

4.1.2 Booster Landing Trajectory Optimization

G-FOLD

Here should be a description of G-FOLD. I just don't know if I should put it into another section or something, but for now, it makes sense to have it here.

4.2 Navigation

The main purpose of navigation is to determine the vehicle's position and orientation in space using a set of sensors. In the case of modern LVs, the sensor set usually consists of a Global Positioning System (GPS) receiver and an Inertial Measurement Unit (IMU) with accelerometers and gyroscopes [17].

Add intro text about sensor fusion if KF is included

4.2.1 Accelerometers

An accelerometer is an inertial sensor that indirectly measures the specific force along to prevent a known proof mass from moving when its case is being accelerated [24]. While the number of different types of accelerometers is large, the basic principle of all of them is the same.

The accelerometer contains a proof mass of known weight that is free to move in the accelerometers' sensitive axis. When an accelerating force acts on the accelerometer case

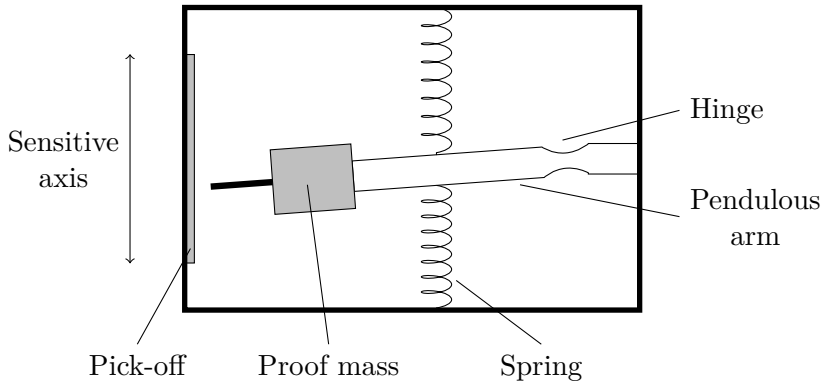

Figure 4.2: Simple mechanical pendulous accelerometer.

in the sensitive axis, the proof mass will not immediately change its velocity. This causes a displacement of the proof mass relative to the case, measured by the pick-off [9].

quartz accelerometer principle

accelerometer math from stevens

4.2.2 Gyroscopes

A gyroscope is an inertial sensor that measures the angular rate around an axis. Unlike accelerometers, there are three main types of gyroscopes, each of which uses a different basic principle [9].

Originally, most gyroscopes were spinning-mass gyros. The basic principle of these gyroscopes employs the conservation of angular momentum. Due to their high complexity, power consumption, and other disadvantages stemming from their mechanical nature, they have been superseded by optical and vibratory gyros [9].

Optical gyroscopes are commonly used in aerospace applications [9, 17]. There are two main kinds: the Ring Laser Gyroscope (RLG) and the Interferometric Fiber-Optic Gyro (IFOG). Both of these employ the same core principle—the *Sagnac effect*.

Change or add credit to myself?

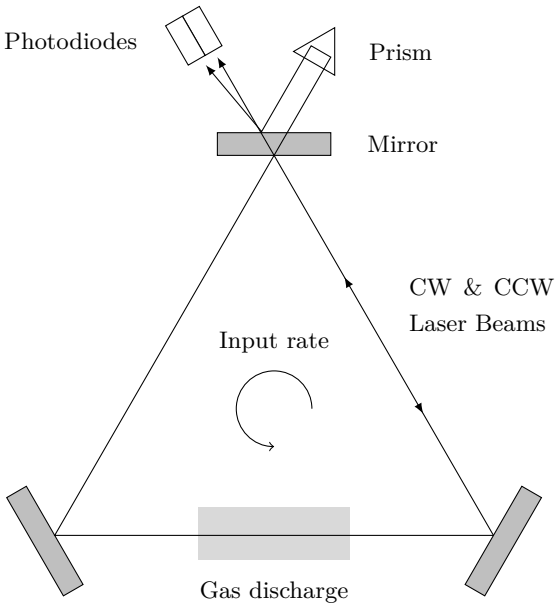

Figure 4.3: The Ring Laser Gyroscope

The Ring Laser Gyroscope (RLG), shown in fig. 4.3, is formed by a (usually) triangle-shaped laser cavity with mirrors in each of the corners. There are two laser beams in the cavity—one in each direction. If the gyroscope is stationary, both beams have the same wavelength. However, if the gyro rotates around its sensitive axis, the path of the beam in the direction of rotation is longer, which results in an increase of the wavelength. The opposite happens for the beam in the other direction [9].

Due to the scattering inside the cavity, the wavelengths of the two beams do not diverge at low angular rates. This issue is resolved in most RLGs by the dither wheel, which applies low-amplitude, high-frequency vibrations around the sensitive axis [9].

The second type of optical gyroscope, the Interferometric Fiber-Optic Gyro (IFOG), was initially developed as a lower-cost solution, but nowadays its performance is on par with the RLG, and its reliability is higher than both RLG and spinning-mass gyro [9].

4.2.3 Global Navigation Satellite Systems

The accuracy of accelerometers and gyroscopes decreases overtime during their use. Fortunately, the launch only takes a few minutes, during which the accumulated error on the sensors is often still acceptable [4]. However, today's missions often require better accuracy, which cannot be reached by IMU alone [17]. Most importantly, such high accuracy is a necessity for the vertical landing of the rocket booster [2]. To achieve the required accuracy, most LVs utilize some kind of Global Navigation Satellite System (GNSS). While there are currently multiple competing satellite navigation systems, the basic principle, which will be described in this section, is the same.

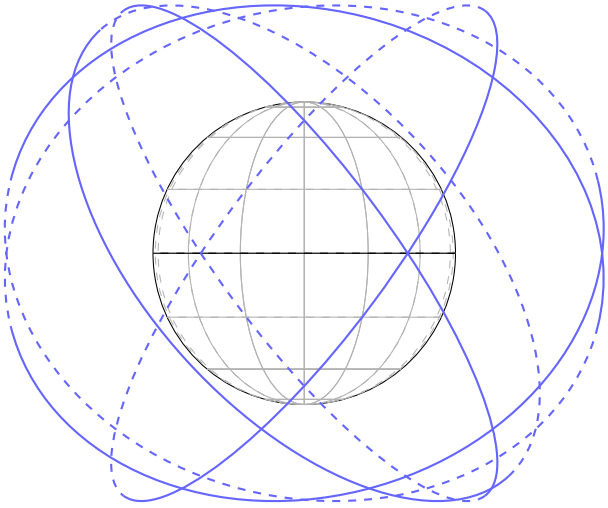

Figure 4.4: Orbital planes of the Global Positioning System (GPS).

Improve figure

A GNSS consists of a large network of satellites, known as a *constellation*, positioned in several orbital planes in a way that ensures the visibility of 5–14 satellites from most places on the Earth at most times, if there is a clear line of sight [9]. Example of such satellite constellation is shown in fig. 4.4.

The satellites broadcast multiple signals with various data. Among them, timing messages and information about satellite orbits, which make it possible to calculate the current position of a satellite [9].

As a result, position of a GNSS receiver can be determined by performing a range measurement from satellite signal by constructing a sphere with radius r (determined from the signal strength) with center in the satellite. The receiver then may lie anywhere in the walls of this sphere. By adding a measurement from a second satellite, the area of possible receiver positions is reduced to intersection of the two spheres—a circle. Third satellite reduces this further to only two points on the circle. This ambiguity can be resolved by adding further measurements, or in some cases by simply eliminating the non-viable point (*e.g.*, when it lies inside the Earth) [9].

Ranging figure

4.2.4 Navigation Filters

4.3 Control

4.3.1 Propulsion

Even though the primary use of the rocket engine is not control, many modern rocket engines are equipped with a Thrust Vector Control (TVC) system, which adds the ability to manipulate the direction of the engine thrust. For this reason, the description of a rocket engine and the TVC is included in this chapter.

A rocket engine produces thrust by ejecting high-temperature propellant gas at high speeds. In accordance with Newton's third law of motion, this causes the motion of a rocket in the direction opposite to the direction of the ejected gas [10].

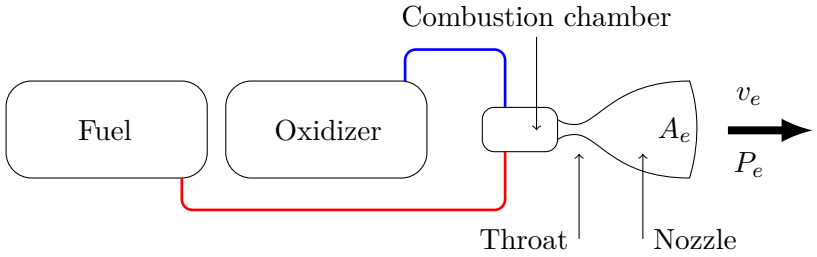

Figure 4.5: Simplified scheme of a liquid bi-propellant engine.

In this work, a liquid bi-propellant rocket engine will be considered, as it is the most common type of rocket engine used for the first stage. As can be seen in fig. 4.5, in these engines, a liquid fuel and oxidizer combines in the combustion chamber.

The hot gas then leaves the combustion chamber and passes through the converging portion of the nozzle, where it is accelerated to sonic speed. To further increase the velocity of the gas, it must be expanded in the diverging part of the nozzle [10].

The thrust of the rocket engine depends on the difference between the exhaust gas pressure P_e and the ambient pressure P_0 around the rocket engine — for ideal performance, the pressures should be equal. The exhaust gas pressure P_e is affected by the cross-sectional area of the exit plane A_e.

These characteristics of a rocket engine can be modeled using the *Thrust equation*:

$$F_t = \dot{m} v_e + A_e(P_e - P_0) \tag{4.1}$$

where F_t is the thrust force of a rocket engine, $\dot{m}$ is the mass flow rate, and v_e is the effective exhaust velocity at the exit plane when $P_e = P_0$.

To control the direction of the thrust, several different methods of TVC exist. For rocket engines, the most common solution is to gimbal the nozzle of an engine. This can be achieved, for example, by fixing the top of the engine to the vehicle through a spherical joint. The direction of the engine is then controlled using two actuators, which are mounted parallel to the pitch and yaw axis of the vehicle [10]. A simplified scheme of such method of attachment can be seen in fig. 4.6.

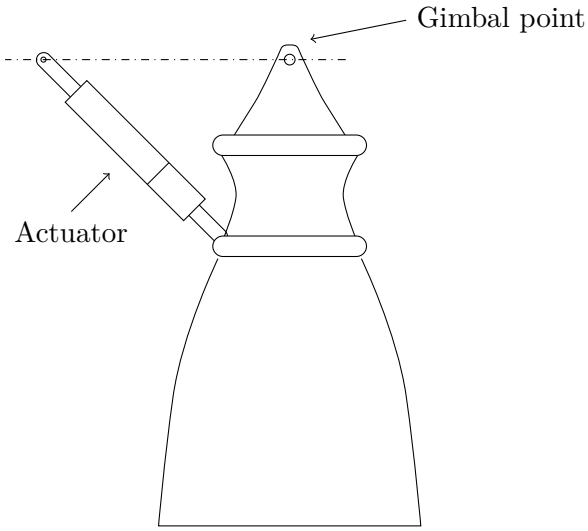

Figure 4.6: Gimbal mechanism of a rocket engine.

figure with engine gimbal and forces/moments

When the engine gimbals, the direction of the thrust changes in the same way. This can be expressed mathematically by rotating the thrust vector (originally coincident with the vehicle $-x$ axis) by angles δ_θ and δ_ψ, which represent the gimbal deflection in the pitch and yaw axes. This can be achieved by constructing a rotation matrix in a similar way as in section 2.1:

$$\vec{F_t} = \begin{bmatrix} F_{t_x} \\ F_{t_y} \\ F_{t_z} \end{bmatrix} = \begin{bmatrix} \cos\delta_\theta \cos\delta_\psi & \sin\delta_\psi & -\sin\delta_\theta \cos\delta_\psi \\ -\cos\delta_\theta \sin\delta_\psi & \cos\delta_\psi & \sin\delta_\theta \sin\delta_\psi \\ \sin\delta_\theta & 0 & \cos\delta_\theta \end{bmatrix} \cdot \begin{bmatrix} F_t \\ 0 \\ 0 \end{bmatrix} = \begin{bmatrix} F_t \cos\delta_\psi \cos\delta_\theta \\ -F_t \cos\delta_\theta \sin\delta_\psi \\ F_t \sin\delta_\theta \end{bmatrix} \quad (4.2)$$

The eq. (4.2) transforms the gimbaled thrust force into the BFF, which is then added to other forces acting on the vehicle. However, gimbaling the engine also produces a rotational moment about the vehicles center of gravity (CG), which also needs to be considered. Considering the forces are applied at the point $\vec{X_{cp}}$ and the center of gravity (CG) is located at point $\vec{X_{cg}}$ (both positions specified in the BFF), the resulting moments can be calculated as [28]:

$$\vec{M_t} = \begin{bmatrix} M_{t_x} \\ M_{t_y} \\ M_{t_z} \end{bmatrix} = \vec{F_t} \times \left(\vec{X_{cg}} - \vec{X_{cp}} \right) \quad (4.3)$$

The gimbal mechanism can only move the engine in the vehicle y and z axes, which means that only pitch and yaw can be controlled with single gimbaled engine. In such cases, the roll control can be achieved using for example with RCS. However, if the stage has two or more gimbaled engines, it is possible to generate torque about the x axis by differentially gimbaling the engines as shown in fig. 4.7 [10].

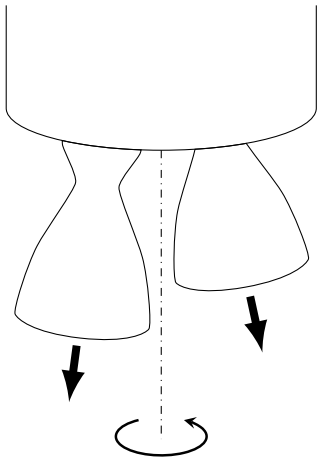

Figure 4.7: Roll control using two gimbaled engines.

4.3.2 Reaction Control System

4.3.3 Grid Fins

Chapter 5

Simulating Launch and Landing

Previous chapters described in detail various aspects that need to be considered to create a model of a rocket itself. However, such a model on its own is not sufficient to create a simulation of the flight, as the rocket is affected by and interacts with its environment during the entire flight. Therefore, the rocket model must be complemented by models of various aspects of the environment, such as gravity or atmosphere, which will be described in this chapter.

5.1 Atmospheric Model

As was mentioned earlier in chapter 3, the LV spends a significant portion of time in the atmosphere during the launch and landing. Thus, the atmosphere plays a significant role during the flight as it affects multiple aspects, such as the aerodynamic forces or performance of the rocket engine.

The properties of the atmosphere, such as temperature, speed of sound, air pressure, and air density are not constant, but are dependant on time and space [21]. These dependencies can be approximately described using an atmospheric model.

One of the most commonly known models is the *U.S. Standard Atmosphere*. It is an idealized steady-state representation of the atmosphere, which uses a set of equations and tables to provide approximations of various parameters of the atmosphere [15]. The full extent of this model exceeds the scope of this work, therefore, only a small subset of these equations will be presented.

The first important parameter provided by the atmospheric model is the temperature. For altitudes up to 86 km, the altitude is given by a series of seven successive equations in the following general form [15]:

$$T = T_{0,b} + L_{M,b}\,(h - h_b) \tag{5.1}$$

where the $T_{0,b}$ for the first layer ($b = 0$) is equal to 288.15 K, and the successive values are obtained from previous calculations of the eq. (5.1). The molecular-scale temperature gradient $L_{M,b}$ and layer reference altitude h_b are given by table 5.1 for each value of b.

The pressure, which is used, for example, in the thrust equation (see section 4.3.1), is given for altitudes up to 86 km by the equation

$$P = P_b \left[\frac{T}{T + L_{M,b}\,(h - h_b)} \right]^{\frac{gM_0}{R^* L_{M,b}}} \tag{5.2}$$

where $P_b = 10132\,\text{Pa}$ is the reference pressure at sea level, g is the gravitational acceleration, $M_0 = 0.028964\,\text{kg}\,\text{mol}^{-1}$ is the molar mass of air at sea level, and R^* is the universal gas constant [15]. The variable $L_{M,b}$ represents molecular-scale temperature gradient, which can be found in table 5.1.

Table 5.1: Atmospheric model variables used for calculation of temperature and pressure [15].

b	h_b	$L_{M,b}$
0	0	−6.5
1	11	0.0
2	20	1.0
3	32	2.8
4	47	0.0
5	51	−2.8
6	71	−2.0
7	84.852	

From the values obtained in eqs. (5.1) and (5.2), the air mass density, which is necessary for the aerodynamic equations, can be simply calculated [15]:

$$\rho = \frac{PM}{RT} \tag{5.3}$$

Lastly, we need to calculate the speed of sound a, which affects the aerodynamic characteristics of the vehicle. The equation used in the *U.S. Standard Atmosphere* model is the following:

$$a = \left(\frac{\gamma R^* T}{M_0}\right)^{\frac{1}{2}} \tag{5.4}$$

where γ is the ratio of specific heat of air at constant pressure, defined to be exactly 1.40 [15]. The speed of sound then can be used to calculate the Mach number for any velocity vector V by using the following equation:

$$Mach = \frac{\sqrt{V \cdot V}}{a} \tag{5.5}$$

While the presented equations apply only for the lower parts of the atmosphere, the *U.S. Standard Atmosphere* provides approximations for altitudes up to 1000 km. The values computed by the atmospheric model for the lower parts of atmosphere can be seen in fig. 5.1.

5.2 Earth Gravity Model

As the reusable rocket booster never leaves Earth's gravity field, gravity has a significant effect on the vehicle during the whole flight. Furthermore, the vertical distance covered by the booster is large enough to necessitate the use of a geopotential model to calculate the gravitational acceleration.

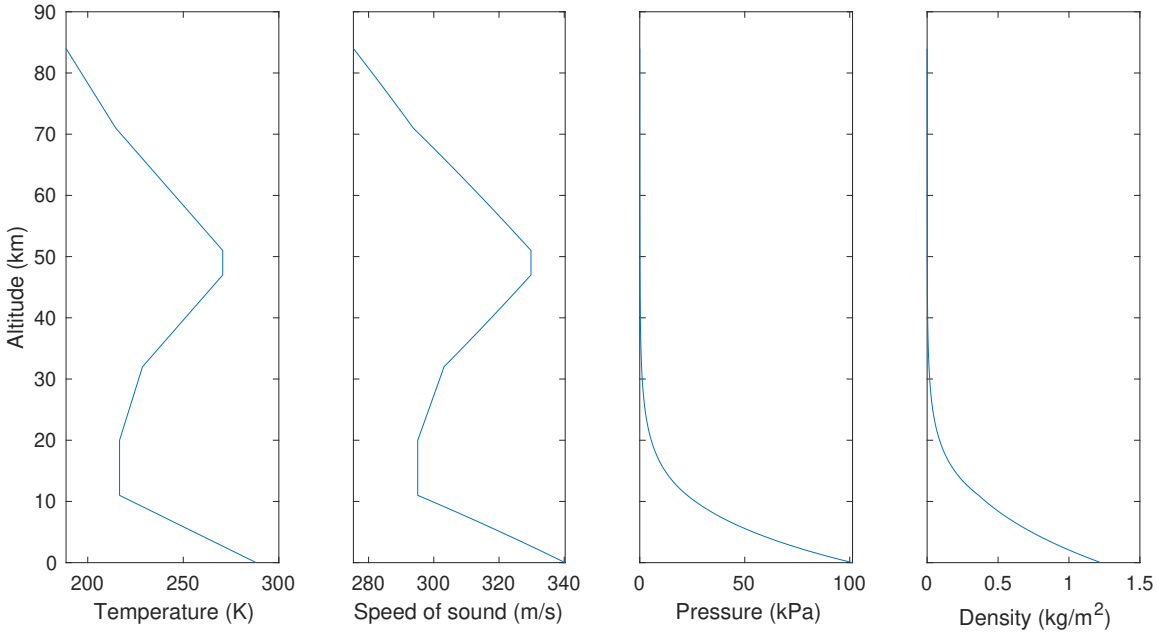

Figure 5.1: Temperature, speed of sound, pressure, and air mass density calculated by the U.S. Standard Atmosphere model for altitudes up to 84 km.

Most of such models are based on a spherical harmonic expansion given by the following expression [7]:

$$U(\Phi,\lambda,h) = \frac{\mu}{r}\left\{-1+\sum_{n=2}^{\infty}\left[\left(\frac{R_E}{r}\right)^n J_n P_{n0}\cos\Phi + \sum_{m=1}^{n}\left(\frac{R_E}{r}\right)^n \left(C_{nm}\cos m\lambda + S_{nm}\sin m\lambda\right) P_{nm}\cos\Phi\right]\right\} \tag{5.6}$$

This equation expresses the gravitational potential $U(\Phi,\lambda,h)$ at a specified latitude Φ, longitude λ, and distance from the center of the planet r, where μ is the standard gravitational parameter of the planet (in the case of Earth, $\mu = 3.986004415\cdot 10^{14}\,\mathrm{m}^3/\mathrm{s}^2$), R_E is the equatorial radius of the Earth, and P_{nm} are Legendre polynomials [7].

Finally, the coefficients J_n, called *zonal harmonic coefficients*, reflect the mass distribution of Earth independently of longitude [7]. Similarly, C_{nm} are the *tesseral harmonic coefficients* for $n \neq m$, and S_{nm} are the *sectoral harmonic coefficients* for $n = m$.

Table 5.2: Approximate values of low-order zonal, tesseral, and sectoral harmonic coefficients from the JGM-3 model [25].

n	J_n
2	-0.1083×10^{-2}
3	0.2532×10^{-5}
4	0.1619×10^{-5}
5	0.2277×10^{-6}
6	-0.5396×10^{-6}

n	m	C_{nm}	S_{nm}
2	1	-0.2414×10^{-9}	0.1543×10^{-8}
2	2	0.1575×10^{-5}	-0.9039×10^{-6}
3	1	0.2193×10^{-5}	0.2680×10^{-6}
3	2	0.3090×10^{-6}	-0.2114×10^{-6}
3	3	0.1006×10^{-6}	0.1972×10^{-6}

The values of these coefficients have been determined mostly experimentally from measurements of Earth-orbiting spacecrafts. As a result, there is a growing number of Earth gravity models with various accuracy [7]. As an example, an extract from the JGM-3 model with approximate values of low-order coefficients is presented in table 5.2.

maybe results or something

5.3 Solving Systems of Ordinary Differential Equations

Consider maybe even appendix

Chapter 6

Implementation

Chapter 7

Results

Chapter 8

Conclusion

This work presents a theoretical base of a master's thesis, which aim is to design a Guidance, Navigation, and Control (GNC) system for the vertical landing of a reusable rocket booster. To achieve this, it is necessary to create a sufficiently accurate model of the rocket booster and the environment it flies in. This requires knowledge of coordinate systems, kinematics, aerodynamics, and other aspects of physics, which enable the development of such a model. Furthermore, this work also describes the design of GNC systems in current spacecraft, which will serve as a basis for building the GNC in this work.

This document is just one part of the work done on this master's thesis. The second part is a prototype model of the booster and environment, created in Simulink. This model has been incrementally developed, starting from a simple basic version, to which more parts were added. Due to the prototypical nature of this model, it was not presented in this document.

Bibliography

[1] *IAU Nomenclature for Fundamental Astronomy*. 2007. Available at: https://syrte.obspm.fr/iauWGnfa/index.html.

[2] Blackmore, L. Autonomous Precision Landing of Space Rockets. *The Bridge*. 2016, vol. 46, no. 4, p. 15–20. ISSN 0737-6278.

[3] Cai, G., Chen, B. M. and Lee, T. H. *Unmanned rotorcraft systems*. New York: Springer, 2011. Advances in industrial control. ISBN 9780857296344.

[4] Davies, M., ed. *The standard handbook for aeronautical and astronautical engineers*. New York: McGraw-Hill, 2003. McGraw-Hill standard handbooks. ISBN 9780071362290.

[5] Dumont, E., Ecker, T., Chavagnac, C., Witte, L., Windelberg, J. et al. CALLISTO - Reusable VTVL launcher first stage demonstrator. 2018. Available at: https://elib.dlr.de/119728/.

[6] Durham, W. *Aircraft flight dynamics and control*. Chichester, West Sussex: John Wiley & Sons, Inc, 2013. ISBN 9781118646786 9781118646793 9781118646809.

[7] Fortescue, P. W., Stark, J. and Swinerd, G., ed. *Spacecraft systems engineering*. 3rd edth ed. New York: J. Wiley, 2003. ISBN 9780470851029 9780471619512.

[8] Grewal, M. S., Weill, L. R. and Andrews, A. P. *Global positioning systems, inertial navigation, and integration*. 2nd edth ed. Hoboken, N.J: Wiley-Interscience, 2007. ISBN 9780470041901. OCLC: ocm70259027.

[9] Groves, P. D. *Principles of GNSS, inertial, and multisensor integrated navigation systems*. 2nd edth ed. Boston: Artech House, 2013. GNSS technology and application series. ISBN 9781608070053. OCLC: ocn820530994.

[10] Iaco Veris, A. de. *Fundamental Concepts on Liquid-Propellant Rocket Engines*. 2021. ISBN 9783030547042.

[11] Jamshed, S. *Using HPC for computational fluid dynamics: a guide to high performance computing for CFD engineers*. Amsterdam: Elsevier/Academic Press, 2015. ISBN 9780128015674. OCLC: ocn918792203.

[12] Jia, Y.-B. Quaternions. *Com S 477/577 Notes*. 2020. Available at: http://web.cs.iastate.edu/~cs577/handouts/quaternion.pdf.

[13] Koks, D. *Using Rotations to Build Aerospace Coordinate Systems*. DSTO-TN-0640. DEFENCE SCIENCE AND TECHNOLOGY ORGANISATION SALISBURY (AUSTRALIA) SYSTEMS SCIENCES LAB, august 2008. Available at: https://apps.dtic.mil/docs/citations/ADA484864.

[14] National Aeronautics and Space Administration. *Project Apollo Coordinate System Standards*. Washington, D.C.: [b.n.], 1965. Available at: http://www.ibiblio.org/apollo/Documents/19700076120.pdf.

[15] National Aeronautics and Space Administration. *U.S. Standard Atmosphere*. NASA-TM-X-74335. 1976. Available at: https://ntrs.nasa.gov/citations/19770009539.

[16] Noureldin, A., Karamat, T. B. and Georgy, J. *Fundamentals of Inertial Navigation, Satellite-based Positioning and their Integration*. Berlin, Heidelberg: Springer Berlin Heidelberg, 2013. ISBN 9783642304651 9783642304668. Available at: http://link.springer.com/10.1007/978-3-642-30466-8.

[17] Oliver, T. E., Park, T., Anzalone, E., Smith, A., Strickland, D. et al. Space Launch Systems Block 1B Preliminary Navigation System Design. In:. 2018. Available at: https://ntrs.nasa.gov/citations/20180002039.

[18] Ortega, G. *ESA Guidance, Navigation and Control Systems*. 2014. Available at: http://www.et.tu-dresden.de/ifa/fileadmin/user_upload/www_files/Aktuelles/2014-01-27_ESA_Guidance__Navigation__and_Control_Systems.pdf.

[19] Pisacane, V. L., ed. *Fundamentals of space systems*. 2nd edth ed. Oxford ; New York: Oxford University Press, 2005. The Johns Hopkins University/Applied Physics Laboratory series in science and engineering. ISBN 9780195162059.

[20] Rose, D. *Quaternions*. 2015. Available at: http://danceswithcode.net/engineeringnotes/quaternions/quaternions.html.

[21] Saha, K. *The Earth's Atmosphere: Its Physics and Dynamics*. Berlin: Springer, 2008. ISBN 9783540784265. OCLC: ocn213114189.

[22] Scott, J. *Lift & Drag vs. Normal & Axial Force*. 2004. Available at: http://www.aerospaceweb.org/question/aerodynamics/q0194.shtml.

[23] Space Exploration Technologies Corp.. *Falcon User's Guide*. 2020. Available at: https://www.spacex.com/media/Falcon_Users_Guide_082020.pdf.

[24] Stevens, B. L., Lewis, F. L. and Johnson, E. N. *Aircraft control and simulation: dynamics, controls design, and autonomous systems*. Third editionth ed. Hoboken, N.J: John Wiley & Sons, 2016. ISBN 9781118870983. OCLC: ocn935444384.

[25] Tapley, B. D., Schutz, B. E. and Born, G. H. *Statistical Orbit Determination*. Amsterdam ; Boston: Elsevier Academic Press, 2004. ISBN 9780126836301.

[26] The Boeing Company. *Space Shuttle Main Engine Orientation*. 1998. Available at: http://large.stanford.edu/courses/2011/ph240/nguyen1/docs/SSME_PRESENTATION.pdf.

[27] The MathWorks, Inc.. *About Aerospace Coordinate Systems - MATLAB & Simulink*. 2020. Available at: https://www.mathworks.com/help/aeroblks/about-aerospace-coordinate-systems.html.

[28] The MathWorks, Inc.. *Aerospace Blockset™ User's Guide*. 2021. Available at: https://www.mathworks.com/help/pdf_doc/aeroblks/aeroblks.pdf.

[29] Wie, B. *Space vehicle dynamics and control*. 2nd edth ed. Reston, VA: American Institute of Aeronautics and Astronautics, 2008. AIAA education series. ISBN 9781563479533. OCLC: ocn232786911.

[30] Zipfel, P. H. *Modeling and simulation of aerospace vehicle dynamics*. 2nd edth ed. Reston, Va: American Institute of Aeronautics and Astronautics, 2007. AIAA education series. ISBN 9781563478758. OCLC: ocm78072255.

List of Acronyms

AoA	Angle of Attack
AoS	Angle of Sideslip
BFF	Body Fixed Frame
CFD	Computational Fluid Dynamics
CG	Center of Gravity
CTP	Conventional Terrestrial Pole
DOF	Degrees of Freedom
ECEF	Earth-Centered, Earth-Fixed frame
ECI	Earth-Centered Inertial frame
FDM	Finite-Difference Method
FVM	Finite-Volume Method
GNC	Guidance, Navigation, and Control
GNSS	Global Navigation Satellite System
GPS	Global Positioning System
IFOG	Interferometric Fiber-Optic Gyro
IMU	Inertial Measurement Unit
LV	Launch Vehicle
NED	North-East-Down
RCS	Reaction Control System
RLG	Ring Laser Gyroscope
TT	Terestrial Time
TVC	Thrust Vector Control
VTVL	Vertical Takeoff, Vertical Landing

List of Symbols

a	Speed of Sound
α	Angle of Attack
A	Axial Force
β	Angle of Sideslip
D	Drag Force
g	Gravitational acceleration
L	Lift Force
m	Mass
$\dot{m}$	Mass flow
N	Normal Force
P	Pressure
Φ, λ, h	Latitude, longitude, and altitude
ϕ, θ, ψ	Roll, pitch, and yaw angles
p, q, r	Rotation rates around the axes
ρ	Density of air mass
$R_a(\alpha)$	Rotation around axis a by angle α
T	Temperature
$\boldsymbol{T}_{\boldsymbol{A}}^{\boldsymbol{B}}$	Transformation from coordinate system $\boldsymbol{A}$ to $\boldsymbol{B}$